Eng. & Tech. Journal, Vol. 30 , No.9, 2012

Plane Flow Analysis for a Profile Extrusion Die Using Digital Image processing Technique

Dr. Salah K. Jawad
Production Engineering & Metallurgy Department, University of Technology / Baghdad
Email: mosaka_2010@yahoo.com
Dr. Ali Abbar Khleif
Production Engineering & Metallurgy Department, University of Technology / Baghdad
Email: aliuot@yahoo.com
Mr. Mohanad Q. Abbood
Production Engineering & Metallurgy Department, University of Technology / Baghdad
Email:mohanad_production@yahoo.com

Received on: 8/9/2011 & Accepted on: 1/3/2012

ABSTRACT

This paper investigates the applicability of the proposed digital image correlation (DIC) system instead of traditional method by microscope to measure the strains in forward extrusion process, which conducted for rectangular section with plane strain condition by using taper die at angle (2α = 90°) and the proportion of reduction in area is (42.85 %). Commercial pure lead (99.99% Pb) was chosen as a typical pattern to measure the strain and strain rate for the forward extrusion process by a visio-plasticity technique and the proposed digital image correlation system. The obtained results indicate that the proposed digital image correlation (DIC) system is an accurate and reliable for measuring the strains using inexpensive equipments.

Keywords: Extrusion Process, Visio-Plasticity, Digital Image Correlation.

تحليل الأنسياب المستوي في قالب بثق بأستخدام تقنية المعالجة الصورية الرقمية

الخلاصة

يتناول هذا البحث قابلية تطبيق نظام مطابقة الصور الرقمية المقترح بدلا من الطريقة التقليدية بأستخدام المجهر لقياس الأنفعال خلال عملية البثق الأمامي، حيث تم إجراء العملية لمقاطع مربعة تحت ظروف الأنفعال المستوي بأستخدام قالب مخروطي بزاوية (2α = 90°) وبنسبة تخصر للمساحة مقدارها (٤٢.٨٥%). تم أختيار الرصاص النقي التجاري (٩٩.٩٩%) كنموذج لأجراء عملية البثق الأمامي ومن ثم قياس الأنفعال ومعدل الأنفعال بأستخدام كل من تقنية اللادونة المرئية ونظام مطابقة الصور الرقمية المقترح في هذا البحث. لقد بينت النتائج المستحصلة دقة ومعولية النظام المقترح لمطابقة الصور الرقمية في قياس الأنفعال بأستخدام معدات غير مكلفة.

INTRODUCTION

Extrusion process is a bulk forming process in which the material is made to flow using high pressure. The movement of the punch and the flow of the material are in the same direction. During the extrusion process the pressure of the punch forces the material to flow in the direction of the movement of the punch, in the process of which the work piece being formed takes the shape of the die inside the container [1].

DIGITAL IMAGE CORRELATION TECHNIQUE

The digital image correlation is an optical technique that uses a mathematical correlation analysis to examine digital image data taken while samples are in mechanical tests. This technique consists of capturing consecutive images with a digital camera during the deformation period to evaluate the change in surface characteristics and understand the behavior of the sample while it is subject to incremental loads. To apply this method, the specimen needs to be prepared by the application of a random dot pattern (speckle pattern) to its surface [2].

This technique starts with a picture before loading (reference image) and then a series of pictures are taken during the deformation process (deformed images). All the deformed images show a different random dot pattern relative to the initial non-deformed reference image. With computer software these differences between patterns can be calculated by correlating all the pixels of the reference image and any deformed image as shown in Figure (1), and a strain distribution map can be created [2].

SOME RELATED WORKS

The visio-plasticity method is used by **Leo Gusel, Rebeka Rudolf,** and **M. Brezocnik [3]** to analyze a cold forward extruded specimen of copper alloy as a function of the stress field. By means of the indicator of the stress state and the effective strain, which are calculated in several points of the extruded specimen, those places are determined where the possibility of cracks is the greatest. On the basis of known values of the stress components it is possible to calculate the indicator of the state of stresses in the individual points of the extruded specimen by means of equation.

Two different techniques were used by **Leo Gusel** and **Rebeka Rudolf [4]** to analyze the distribution of the effective strain in cold forward extruded copper alloy; the visio-plasticity method, which is used to find the complete stress and strain distribution in the deformation zone, and the second method being micro-hardness technique. An approximation for the relation between micro-hardness and effective strain was determined by polynomial regression analysis. For determination of the impact of friction on the effective strain two different lubricants were used.

Leo Gusel, Rebeka Rudolf, and **B. Kosec [5]** used the visio-plasticity method to find the complete velocity and strain rate distributions from the experimental data, using the finite-difference method. The data

about values of strain rates in plastic region of the material is very important for calculating stresses and the prediction of product quality. Specimens of copper alloy were extruded with different lubricants and different coefficients of friction and then the strain rate distributions were analyzed and compared. Significant differences in velocity and strain rate distributions were obtained in some regions at the exit of the deformed zone.

A. E. Lontos, et al [6] studied the effect of extrusion parameters (extrusion speed and temperature) and die geometry, i.e. extrusion radius, on the extruded billet quality (Equivalent stress and strain) using FEM technique. For this purpose the general FEA software Deform-2D has been used to set up the finite element model of the warm aluminum extrusion in two dimensions. 6061 Aluminum with 40mm diameter and 50mm length was used as billet material. The extrusion process was modeled as isothermal, which means that the billet material was preheated at a specific temperature and then it was pressured into the circular die, with extrusion ratio 3.3. The extrusion speed was varied from 1 to 3 mm/s, the extrusion temperature varied from 400^{o}C to 500^{o}C and the extrusion die radius was varied from 1 to 4 mm. The friction between i) workpiece and die, is related to Coulomb model with 0.3 friction factor, ii) workpiece and stem, is related to Shear model with 0.9 friction factor and iii) workpiece and container, is related to Shear model with 0.96 friction factor. Optimized algorithms for extrusion parameters were proposed regarding to the concluded simulating results.

Leo Gusel and **Rebeka Rudolf [7]** investigate the measurements of velocity fields and impact of friction on velocity distribution in forward extruded specimens of copper alloy using the visio-plasticity method. The visio-plasticity method is used to find the complete velocity distributions from the experimental data by the finite-difference method. Comparison is made between velocity distributions in the specimens extruded with different lubricants with different coefficients of friction. The results in a form of diagrams have shown that the influence of the lubricant's coefficient of friction on the velocity distributions in extruded material can be of great importance especially in some critical regions in the cold formed material.

D. V. R. Murty and **M. Ramulu [8]** studied the plastic deformation characteristics of Dual Channel Lateral Extrusion with FEA. It is observed that the plastic deformation behavior is more complex and the strain induced is highly localized. The extrusion force required is compared with the upper bound value published in literature. It is found from analysis that the strain is inhomogeneous and non uniform.

Leo G. and **Rebeka R. [9]** used visio-plasticity method to analyze velocity fields in forward extruded specimens of copper alloy CuCrZr. The visio-plasticity method is used to find the complete velocity and strain rate distribution from the experimental data by using finite-difference method. Finding out the values of stain rates in plastic region of the material is very important for calculating stresses and prediction of specimen quality.

Comparison is made between velocity distributions in the specimens extruded with three different lubricants with different coefficients of friction. The results in a form of diagram have shown that the influence of the lubricant on the velocity distributions in extruded material can be of great importance especially in some critical regions in the cold formed material.

EXTRUSION RIG

In this work a forward extrusion rig for rectangular sections was designed and manufactured, which is consists of the following main parts: container, ram, pressure pad, and die as shown in Figure (2).

MATERIAL USED

The billet material used in this study for extrusion process is (99.99%) commercially pure lead and its chemical composition listed in Table (1). Lead can be used as a model for a number of metals at different strain rates and temperatures because of similarities in terms of Stress-Strain curves. This is useful in the study of flow metal in the forming processes. As well as its ability to re-crystallization at room temperature its composition is similar to the hot forming process for steel which leads to the absence of strain hardening in this metal. Lead has yield stress which varies in amount between (6-8 MPa) and the temperature melting point is (327 °C) [10].

PRINTING THE SQUARE GRIDS

The study of metal flow in metal forming processes requires a grid printing on the meridian plane or separation surface between the two split parts of the testing billets. The grid may be as parallel lines or square grid lines or circular grid based on the specified metal forming process and its requirements for the parameters, which will be studied. The square grid is printed with dimensions of (4.2×4.2 mm) and a depth of about (0.1 mm) by using scratching style after installing the billet on table of vertical milling machine. By using special tool made of HSS which is fixed in axis of the machine. The table (with billet) was moved in longitudinal direction to print the horizontal lines. Following the completion of scratching the table was moved in transversal direction to print the vertical lines. Taking into account in printing the grid as much as possible it to be scratching line was taken as centre for horizontal lines. To make the displacement measuring process easy after the deformation process, upper half of the billet was taken which also represents the displacement in lower half of billet.

And after the completion of samples preparation two billets, were integrated one of them has square grid and the other without the grids. Interval surface between them was sprayed with graphite to ensure that there is no adhesion between billets after the extrusion process. After testing the billets, they were separated from each other and the grid distorted was studied.

THE USE OF VISIO-PLASTICITY TECHNIQUE IN EXTRUSION PROCESS

In this section we will deal with theoretical considerations for Visio-plasticity technique, which is used to determine the strain and strain rates in the extrusion process.

The general two dimensional state of strain at some point of grid is represented by the shown infinitesimal element (dx, dy), where u and v are the x and y-displacements at point A', respectively, and lines A'C' and A'B' have been extended and displaced, as shown in Figure (3).

$$\varepsilon_x = \frac{A'B' - AB}{AB} = \frac{\left[dx + \left(U + \frac{\partial U_x}{\partial x}dx\right) - U\right] - dx}{dx} = \frac{\partial U_x}{\partial x} \quad \ldots (1)$$

$$\varepsilon_y = \frac{A'C' - AC}{AC} = \frac{\left[dy + \left(V + \frac{\partial V_y}{\partial y}dy\right) - V\right] - dy}{dy} = \frac{\partial V_y}{\partial y} \quad \ldots (2)$$

The shear strain consists of the summation slope (U_x) with the y-axis and the slope (V_y) with the x-axis.

$$Y_{xy} = \frac{\partial U_x}{\partial y} + \frac{\partial V_y}{\partial x} \quad \ldots (3)$$

The normal strain and shear strain rates are found by dividing each one of them by(ΔT).

$$\dot{\varepsilon_x} = \frac{\partial Ux}{\partial x} \cdot \frac{1}{\Delta T} \quad \ldots (4)$$

$$\dot{\varepsilon_y} = \frac{\partial Vy}{\partial y} \cdot \frac{1}{\Delta T} \quad \ldots (5)$$

$$\dot{\gamma_{xy}} = \left(\frac{\partial Ux}{\partial y} + \frac{\partial Vy}{\partial x}\right) \cdot \frac{1}{\Delta T} \quad \ldots (6)$$

Since the extrusion process in plane strain, the effective strain rates are calculated from the following relationship [11].

$$\dot{\bar{\varepsilon}} = \frac{2}{3}\left(\left(\dot{\varepsilon_x}^2 + \dot{\varepsilon_y}^2 - \dot{\varepsilon_x}\dot{\varepsilon_y}\right) + \frac{3}{4}\dot{Y_{xy}}^2\right)^{\frac{1}{2}} \quad \ldots (7)$$

TESTING PROCEDURE

Forward extrusion tests on pure lead billets were carried out on the Instron device with capacity of (20 ton). Before the test, a layer of graphite is to be applied to the separation surface of the billet to eliminate the adhesion of both parts. Another sliding parts and container bore were oiled to facilitate the sliding of these parts and to reduce the frictional effects. The set of extrusion rig is then put on the table of the Instron device as shown in Figure (4) and turn on the system with constant speed (V = 10 mm/min) for all tests. The magnitude of the applied extrusion load was

recorded against the punch displacement at equal intervals until the load reaches a steady state condition; it was between 13 and 17 mm, as shown in Figure (5). After finishing the test, the extruded sample is extracted from the container carefully. Then the two parts of the extruded sample are separated carefully and cleaned them from the graphite layer by using a soft piece of cloth for preparation of capturing by the digital camera as will be illustrated in the next paragraphs.

CAPTURING THE DEFORMED EXTRUSION SAMPLES

The proposed DIC system is an optical and non-contact technique for full-field strain measurement which can measure displacements and strains in extrusion sample. To achieve successful correlation between any compared two images, it is necessary to have a grid on the sample surface. A picture of the grid on the sample before and after the extrusion process was captured using digital camera (SONY DSC-W300) with resolution of 13.6 Mega Pixels. MATLAB package, where the image processing toolbox is used to investigate the relative displacement and the surface strains by the use of distinct grid on the sample. Camera calibration is necessary to convert the measurement with pixel unit into metric. We simply used one scale factor along x-direction under the assumption that the image plane and the specimen are parallel. This scale factor is computed by hand using the saved image after loading the specimen. The ratio between pixel counts corresponding to the gauge length on the image and the actual length of the gauge is used as the scale factor.

RESULTS AND DISCUSSION

The algorithm proposed in this work greatly depends on reading out the colored reference extrusion sample image and the colored target extruded image, which are captured using ambient light only to minimize possible illumination noise, and then reducing image information by converting them into gray-scale images as shown in Figure (6-a) and (6-b) respectively.

Gray-scale images are still inhibit much information and are very noisy due to the different brightness intensities, so in order to eliminate these effects a threshold operation is applied to both reference and target gray-scale images. Thus the output image will be a one bit per pixel image named binary image. Accordingly, this image data became simple and ready to compute each pattern pixel displacement as shown in Figure (7) which presents the overlapping of both reference and target images, where it found that each (97 pixels) equal to (12.6 mm) .

Figure (7) shows that the sample was extruded well and there are no twists or deviations in this sample and this indicate that the process has been uniform and correct. Moreover this picture shows that there is curvature in vertical lines on x-axis and the peak of flow is located on the line (Y = 0) which is the center line. The reason for the appearance of this curvature is the existence of variation in the velocities of each point in the flow lines as the speed increases as we move to the center of the sample

and decreases toward the sample surface. This is because of the friction between the sample extruded and the die.

Figure (8) shows the change in horizontal component which remain stationary in the direction of x-axis of the rigid zone. After this zone, and the die enters (the forming zone), component (U_x) begins to increase gradually until it reaches the maximum value at the exit of the die where it remains constant. It is noted the flow line (Y = 21) has different behavior because the horizontal component has a negative value because of friction between the sample and the die wall which hinders the movement of the grains which come under compression in the x-axis. After leaving the forming zone, the horizontal component begins to increase in value.

Figure (9) reveals the change in horizontal component (U_x) in y- axis. It is seen the value of the horizontal component (U_x) changes gradually in value with y-axis. It has maximum value at the center and decreases at it moves towards the surface. This results from friction as stated previously.

Figure (10) shows the change of the vertical component (V_y) with x-axis. It is seen the values of (V_y) on the surface of sample (Y = 21) are high and begins to decrease as it moves towards the center until it reaches the center line where the values of (V_y) are equal to zero. No displacement occurs at the center line towards y-axis. It is notes the values of (V_y) in the forming zone begin to increase in the direction of x-axis for all flow lines until they reach almost equal values except the line in contact with die wall. It is seen its behavior is different because of it's the high deformation. Which hinders its grain movement because of friction, resulting in increase in the vertical displacement between grains laying on the line to the die wall and the line adjacent to it therefore its value is high until it is close to forming zone. The value of (V_y) begins to decrease because of the constriction. It remains close to other flow lines when leaving the forming zone for the y-axis.

Figure (11) shows the change in the vertical component (V_y) with y-axis. The highest value is at the sample surface and begins to decrease towards y-axis. It reaches the lowest value at flow line at the center of the sample (V_y =0).

Figure (12) presents change in horizontal strain rates ($\dot{\varepsilon}_x$) according to equation (4), with x-axis. It is seen that at forming zone the highest value of strain rates is at the center (Y = 0) because friction is low and begins to decrease gradually in the direction of y-axis until it reaches its lowest value at flow line in contact with the die wall (Y = 21). It is noted that at a short distance after entry the value of ($\dot{\varepsilon}_x$) increases in the direction of x-axis because of increase in constriction and it remains constant at the exit point of the die and it remains constant shortly after leaving the forming zone. This behavior occurs with a flow lines except line (Y = 21) which is constant with die wall at which friction is at highest value possible, hindering the grain movement at die entry. Therefore, the particles come under compression in the x-axis direction. The strain values are negative when reaching almost the middle of forming zone, the value of ($\dot{\varepsilon}_x$) begins to reverse because friction is reduced as it moves towards the exit because

the contact area between the extruded sample and die wall is reduced; making the grains move faster and $(\dot{\varepsilon}_x)$ value becomes positive when it exits the forming zone.

Figure (13) reveals the change in vertical strain rates $(\dot{\varepsilon}_y)$ according to equation (5), with x-axis. It is noted that the value of $(\dot{\varepsilon}_y)$ at center line is zero because there is no displacement in y-direction. It is seen that the highest value of $(\dot{\varepsilon}_y)$ is at (Y=8.4). It is also noted that the value of $(\dot{\varepsilon}_y)$ in the x-axis direction after entering the zone begins to increase with increase in constriction until it reaches the exit point at a constant value. All flow lines meet at close points.

Figure (14) shows the change in effective strain rates $(\dot{\bar{\varepsilon}})$ according to equation (7), with x-axis. It is noted that when the x-axis is kept constant, the highest value of effective strain rate is at a line close to the center line. Its lowest value is at flow line (Y=16.8). When it is x-axis direction, its value begins to increase after it enters the forming zone until it reaches the highest value shortly before exiting the forming zone. It continues in this value until it exits the die.

Figure (15) shows the change in shear strain rates $(\dot{\gamma}_{xy})$ according to equation (6), with x-axis. It is seen that the value of shear strain rates $(\dot{\gamma}_{xy})$ in the forming zone is as low as possible at flow line in contact with the die wall (Y = 21). The value increases towards sample center because friction value is low. Speed increases until it reaches its highest value at flow line (Y=4.2).

The shear strain value $(\dot{\gamma}_{xy})$ is the lowest in the direction of x-axis and at zone entry but it increases as it goes in the direction of x-axis because constriction increases. The shear value reaches its highest value at the exit of forming zone.

CONCLUSIONS

On the basis of this study, and observations obtained experimentally, the following findings can be concluded:

- The selection of threshold value of an image is very critical since it affects the representation of sample in the scene. The probability of representing the sample pixels as background pixels leads to loss of some of sample information, thus affecting the measurement accuracy of the proposed system.
- The strains can be measured in extrusion processes by using the proposed DIC system instead of using the traditional method based on the microscope which is required skilled operator.
- Using the conducted experiments for strain measurements in extrusion processes, one can observe that the proposed DIC system is easier and faster than the traditional method using the microscope.

- The proposed measurement set-up is easy and doesn't need special equipments, so the proposed DIC system can be considered as a low-cost method. The accuracy and power of the method are high and open new fields of practical applications in material testing.

REFERENCES

[1]Tschaetsch, H., "***Metal Forming Practice***", Seven Edition, Verlag Berlin Heidelberg, 2006.

[2]Cintrón, R. and Saouma, V., "***Strain Measurements With The Digital Image Correlation System Vic-2D***", Center for Fast Hybrid Testing, Department of Civil Environmental and Architectural Engineering, University of Colorado, Boulder, 2008.

[3]Gusel, L., Rudolf, R., and Brezocnik M., "***An Experimental Research of Formability of Cold Formed Material***", 5th International DAAAM Baltic Conference, Industrial Engineering – Adding Innovation Capacity of Labour Force and Entrepreneurs, Estonia, pp. 261-266, 2006.

[4]Gusel, L. and Rudolf, R., "***Different Techniques for Strain Analysis in Metal Forming Processes***", 6th International DAAAM Baltic Conference, Industrial Engineering, Estonia, 2008.

[5]Gusel, L., Rudolf, R., and Kosec B., "***Analysis of a Strain Rate Field in Cold Formed Material Using the Visioplasticity Method***", Metallurgical, Vol. 48, No. 2, pp. 103-107, 2009.

[6]Lontos, A. E., et al, "***Effect of Extrusion Parameters and Die Geometry on the Produced Billet Quality Using Finite Element Method***", Proceedings of the 3rd International Conference on Manufacturing Engineering, pp. 215-228, 2008.

[7]Gusel, L. and Rudolf, R., "***Research and Measurements of Velocity Field During Extrusion Process***", XIX IMEKO World Congress, Fundamental and Applied Metrology, Portugal, pp. 2383-2387, 2009.

[8]Murty, D. V. R. and Ramulu, M., "***Deformation Study of Equal Channel Lateral Extrusion Using FEM***", International Journal of Engineering Studies, ISSN 0975-6469 Vol. 1, No. 3, pp. 161-168, 2009.

[9]Gusel, L. and Rudolf, R., "***An Experimental Study of Velocity Distribution in Formed Material***", Association of Metallurgical Engineers of Serbia, Vol. 14, No. 3, pp. 201-207, 2008.

[10]Hussein, E. A., "***Study the Geometry Effect of the Die in the Flow of Metal in the Pipe Extrusion Process Technology Followers of Visio-plasticity***", M.Sc. Thesis, Department of Production and Metallurgy Engineering, University of Technology, Baghdad, Iraq, 2006. (In Arabic)

[11]Yajnik, K. S. and Frisch, J., "***Strain Rate Distribution During Experimental Metal Rolling***", J. Eng. Ind. Trans. ASME, pp. 81-88, 1962.

Table (1)The chemical composition of the lead billet

Element	Sb %	Cu %	Mn %	Zn %	Pb %	Fe %	Cd %	Ni %
%	0.002	0.003	0.00005	0.002	99.99	0.001	0.00005	0.001

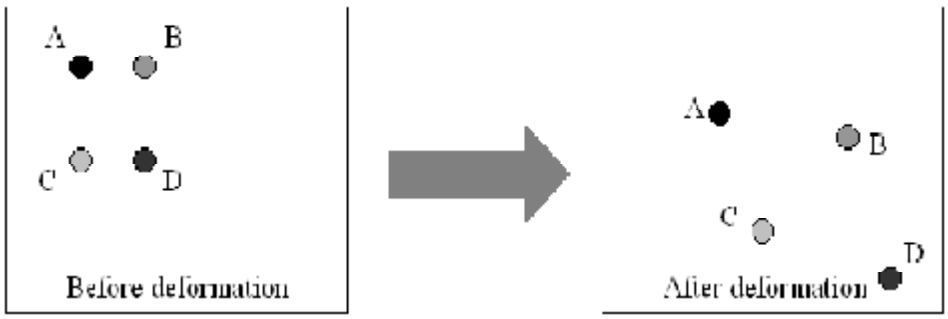

Figure (1) Illustrate, reference pixels before and after deformation. [2]

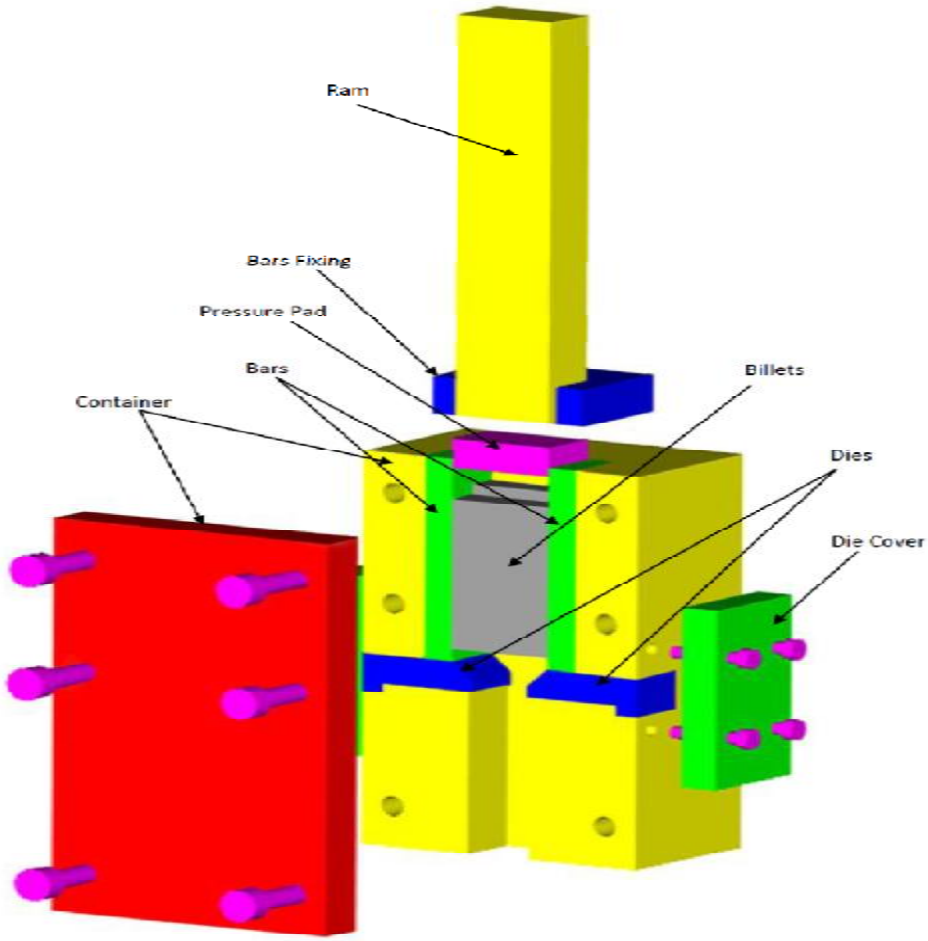

Figure (2) the extrusion rig

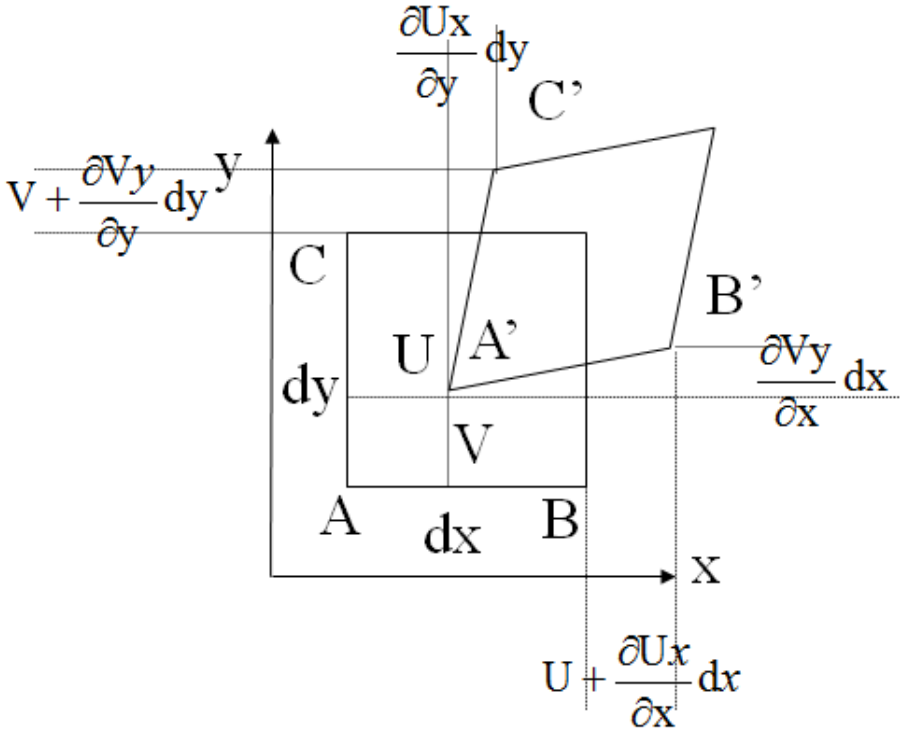

Figure (3)Analysis for grid points in plane strain condition.

Figure (4)The extrusion rig on the Instron device

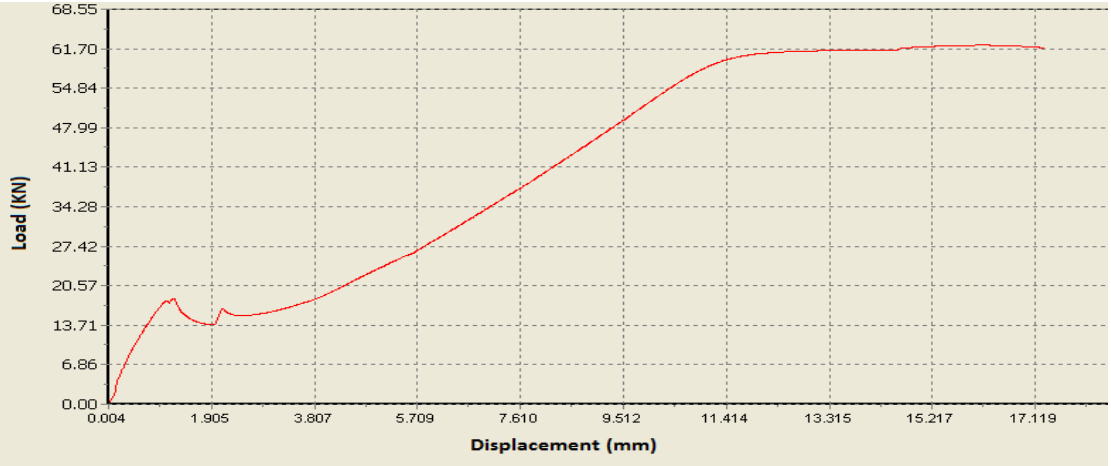

Figure (5)The relationship between the load and the displacement of ram

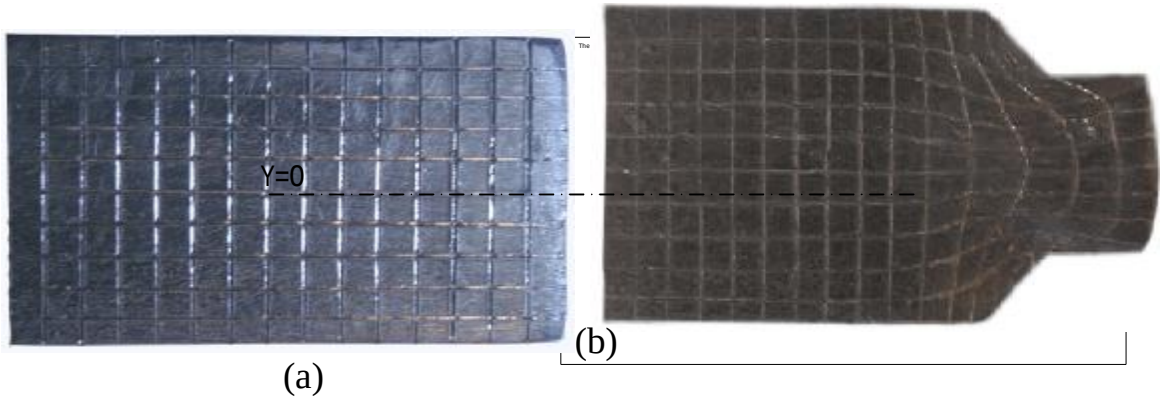

Figure (6) the photograph for the test sample
a) Before and b) after extrusion process

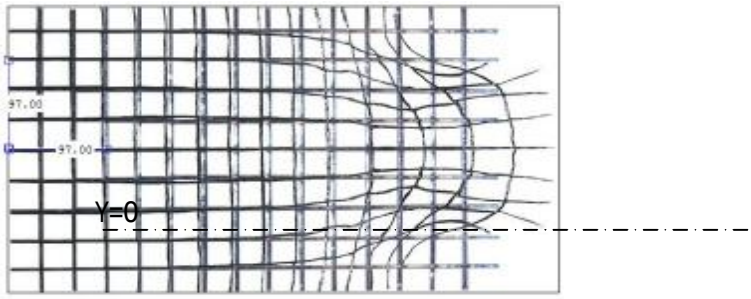

Figure (7)Applying the proposed measuring method on the overlapping images,

where it found that each (97 pixels) equal to (12.6 mm)

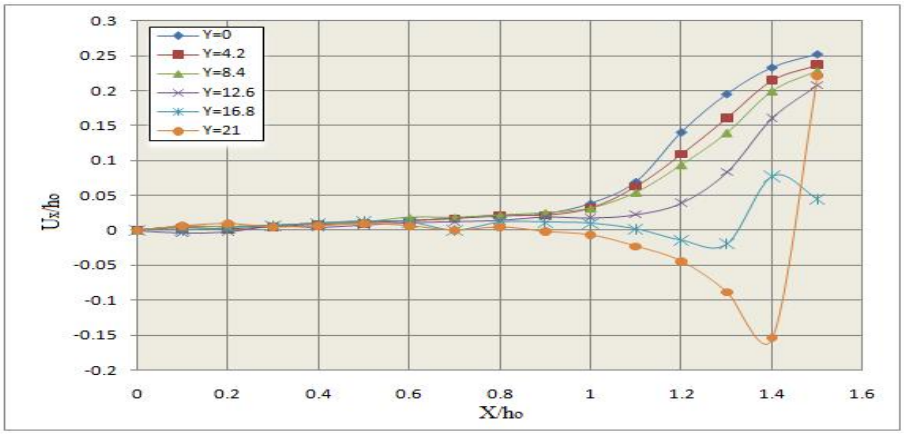

Figure (8)The change in horizontal component (Ux/ho) with the dimension (X/ho)

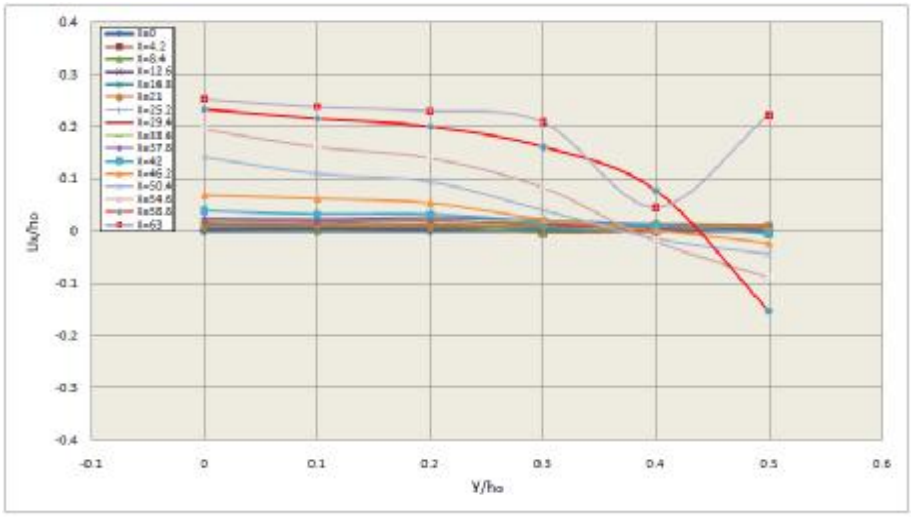

Figure (9)The change in horizontal component (Ux/ho) with the dimension (Y/ho)

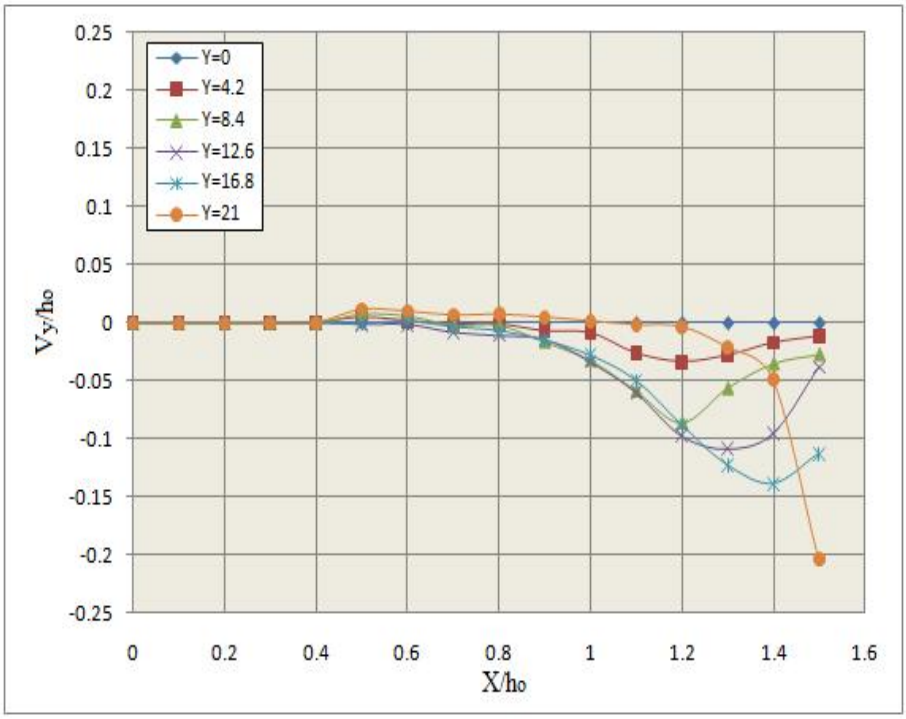

Figure (10)The change in vertical component (Vy/ho) with the dimension (X/ho)

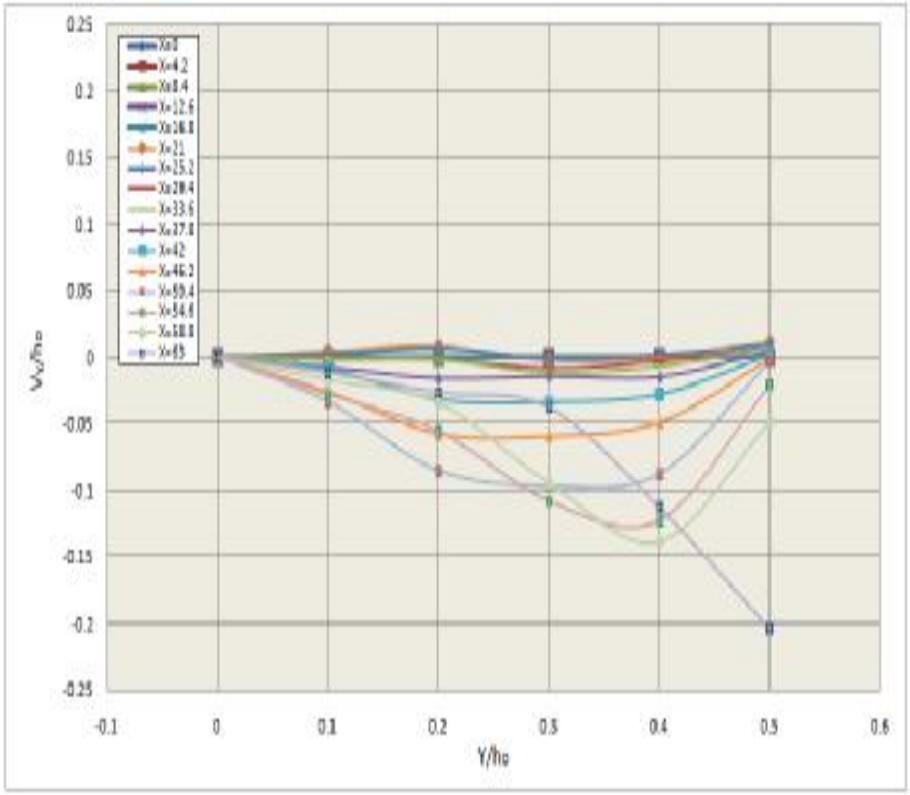

Figure (11)The change in vertical component (Vy/ho) with the dimension (Y/ho)

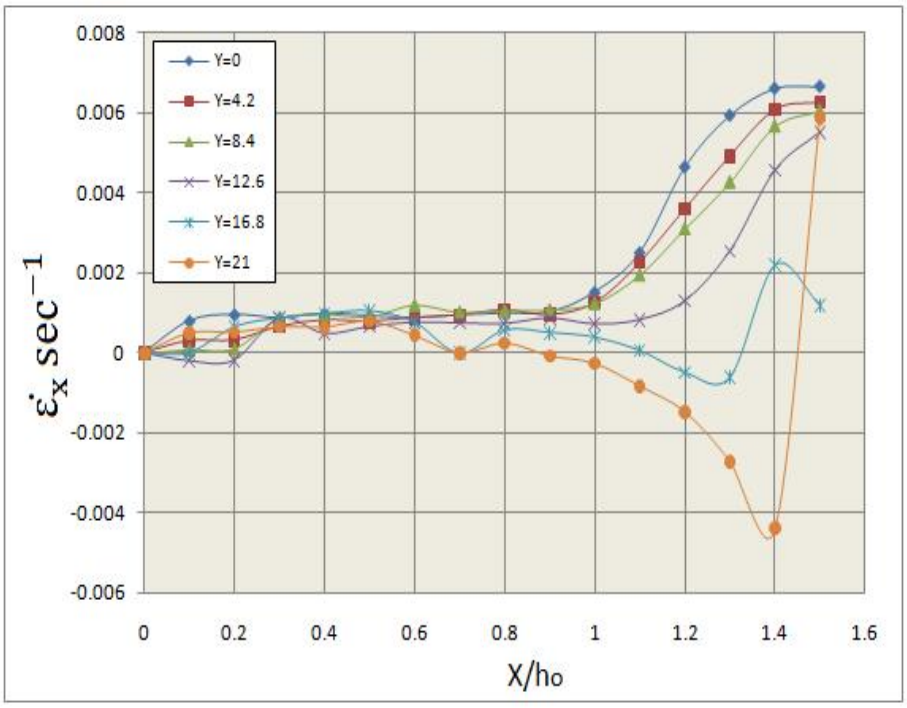

Figure (12)The change in horizontal strain rates ($\dot{\varepsilon}_x$) with the x-axis (X/ho)

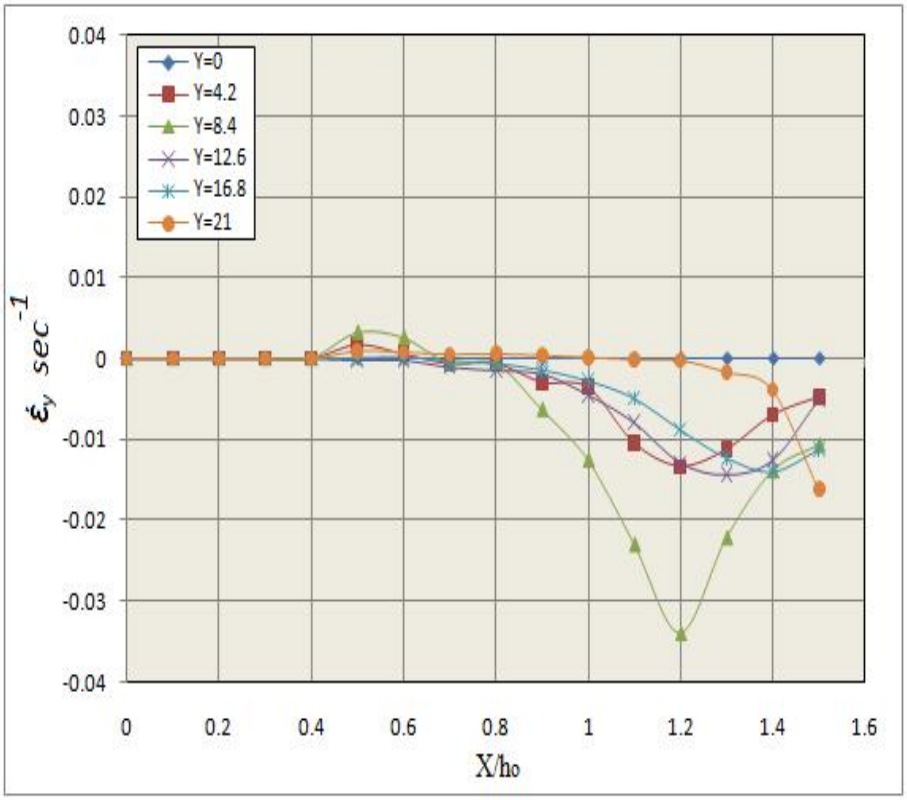

Figure (13)The change in vertical strain rates ($\dot{\varepsilon}_y$) with the x-axis (X/ho)

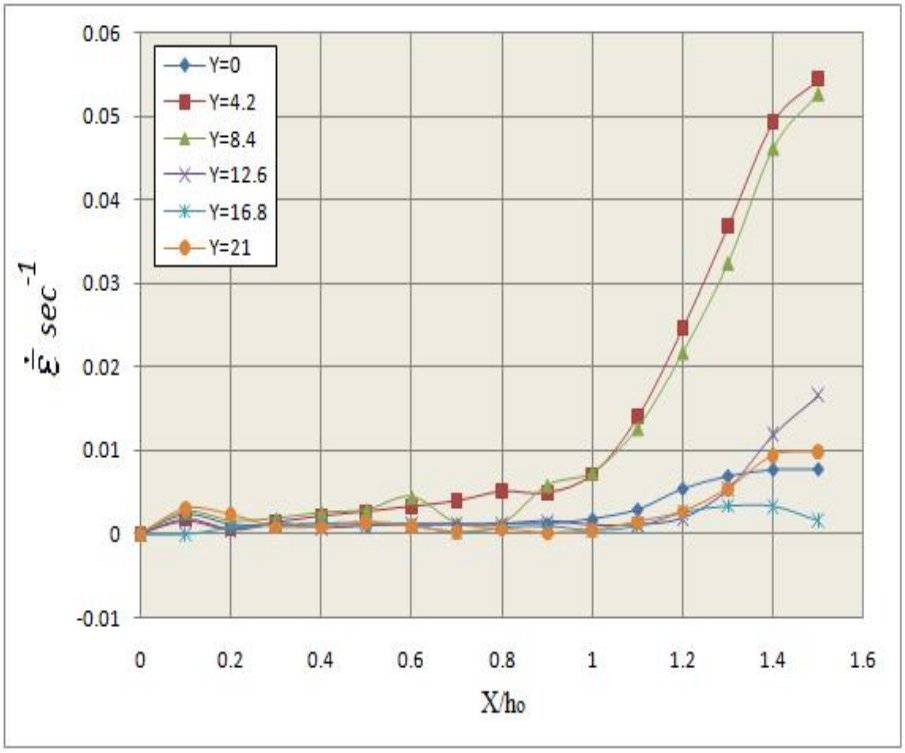

Figure (14)The change in effective strain rates ($\dot{\bar{\varepsilon}}$) with the x-axis (X/ho)

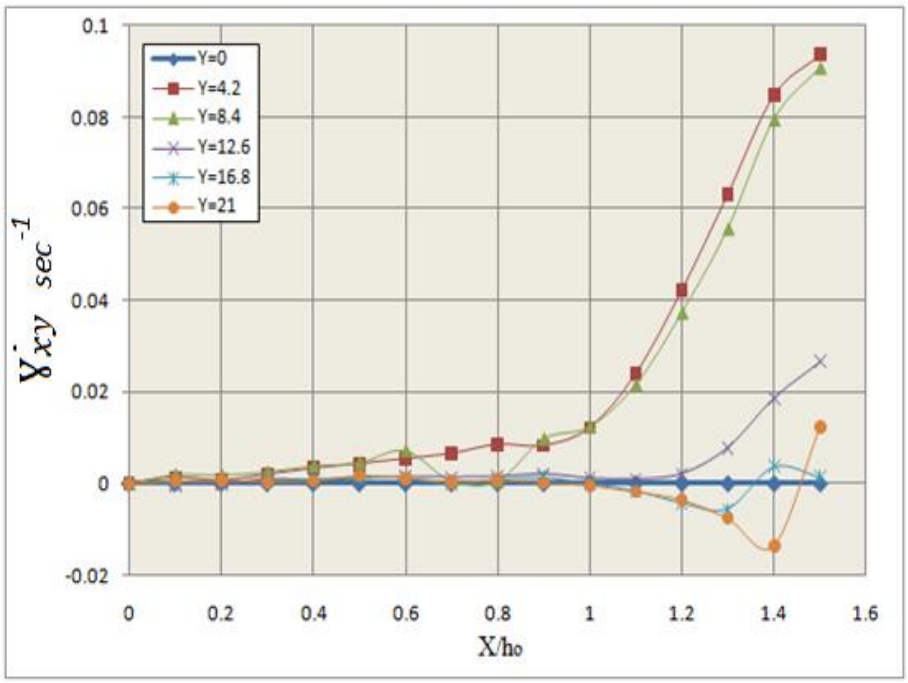

Figure (15)The change in shear strain rates ($\dot{\gamma}_{xy}$) with the x-axis (X/ho)